

# Eight new radio pulsars in the Large Magellanic Cloud

J. P. Ridley,<sup>1</sup>★ F. Crawford,<sup>2</sup> D. R. Lorimer,<sup>3,4,5</sup> S. R. Bailey,<sup>6</sup> J. H. Madden,<sup>2</sup>  
R. Anella<sup>2</sup> and J. Chennamangalam<sup>3</sup>

<sup>1</sup>Department of Engineering and Physics, Murray State University, Murray, KY 42071, USA

<sup>2</sup>Department of Physics and Astronomy, Franklin and Marshall College, Lancaster, PA 17604, USA

<sup>3</sup>Department of Physics, West Virginia University, PO Box 6315, Morgantown, WV 26506, USA

<sup>4</sup>National Radio Astronomy Observatory, PO Box 2, Green Bank, WV 24944, USA

<sup>5</sup>Astrophysics, University of Oxford, Denys Wilkinson Building, Keble Road, Oxford OX1 3RH, UK

<sup>6</sup>Aerospace Engineering Program, Syracuse University, 263 Link Hall, Syracuse, NY 13244, USA

Accepted 2013 April 23. Received 2013 April 23; in original form 2013 March 7

## ABSTRACT

We present the discovery of eight new radio pulsars located in the Large Magellanic Cloud (LMC). Five of these pulsars were found from reprocessing the Parkes Multibeam Survey of the Magellanic Clouds, while the remaining three were from an ongoing new survey at Parkes with a high-resolution data acquisition system. It is possible that these pulsars were missed in the earlier processing due to radio frequency interference, visual judgment or the large number of candidates that must be analysed. One of these new pulsars has a dispersion measure of  $273 \text{ pc cm}^{-3}$ , almost twice the highest previously known value, making it possibly the most distant LMC pulsar. In addition, we present the null result of a radio pulse search of an X-ray point source located in SNR J0047.2–7308 in the Small Magellanic Cloud (SMC). Although no millisecond pulsars have been found, these discoveries have increased the known rotation-powered pulsar population in the LMC by more than 50 per cent. Using the current sample of LMC pulsars, we used a Bayesian analysis to constrain the number of potentially observable pulsars in the LMC to within a 95 per cent credible interval of  $57\,000_{-30\,000}^{+70\,000}$ . The new survey at Parkes is  $\sim 20$  per cent complete, and it is expected to yield at most six millisecond pulsars in the LMC and SMC. Although it is very sensitive to short period pulsars, this new survey provides only a marginal increase in sensitivity to long periods. The limiting luminosity for this survey is  $125 \text{ mJy kpc}^2$  for the LMC which covers the upper 10 per cent of all known radio pulsars. The luminosity function for normal pulsars in the LMC is consistent with their counterparts in the Galactic disc. The maximum 1400 MHz radio luminosity for LMC pulsars is  $\sim 1000 \text{ mJy kpc}^2$ .

**Key words:** stars: neutron – pulsars: general – Magellanic Clouds.

## 1 INTRODUCTION

Our nearest galactic neighbours, the Large and Small Magellanic Clouds (LMC and SMC), are irregular galaxies with a different star formation history than the Milky Way. They therefore represent very interesting targets for pulsar searches. Previous pulsar surveys of the Magellanic Clouds by McCulloch et al. (1983), McConnell et al. (1991), Crawford et al. (2001) and Manchester et al. (2006) have discovered 13 radio pulsars in the LMC. In addition, two rotation-powered X-ray pulsars have been discovered (see Seward, Harnden & Helfand 1984; Marshall et al. 1998), leading to a total of 15 known rotation-powered LMC pulsars. Five radio pulsars were also discovered in the SMC in the surveys by McConnell

et al. (1991), Crawford et al. (2001) and Manchester et al. (2006), yielding a total of 20 rotation-powered pulsars in the Magellanic Clouds.

Pulsar surveys with the Parkes 20-cm Multibeam Receiver (Staveley-Smith et al. 1996) have been carried out along the plane of the Galaxy (Manchester et al. 2001), at intermediate (Edwards et al. 2001) and high Galactic latitudes (Jacoby et al. 2003; Burgay et al. 2006), and in the Magellanic Clouds (Manchester et al. 2006). These surveys have been very successful. Improved computer processing capabilities and search algorithms have inspired a reprocessing of these various Parkes Multibeam Surveys, most notably the Galactic plane survey, and have led to a large number of additional discoveries (Keith et al. 2009; Mickaliger et al. 2012; Eatough et al. 2013; Knispel et al. 2013). In this paper, we present the discovery of five new radio pulsars in the LMC from a reanalysis of the Manchester et al. (2006) survey data and three from a high-resolution survey of

★ E-mail: jridley@murraystate.edu

the LMC which we are conducting at Parkes for a total of eight new radio pulsars.

In Section 2, we introduce the searches that were performed. In Section 3, we explain the data reduction stage, including the dispersion measure (DM), period ( $P$ ) and acceleration search ranges. Our results are then presented in Section 4. We discuss the implications of our results in Section 5, and finally, in Section 6, we draw our conclusions.

## 2 OVERVIEW OF THE SEARCHES

Five separate searches using both new and archival data were performed in order to detect new radio pulsars in the SMC and LMC. Data from the Parkes Multibeam Survey of the Magellanic Clouds (Manchester et al. 2006) were reprocessed and searched using three different sets of search parameters. The first pass focused on low DMs (up to  $300 \text{ pc cm}^{-3}$ ) and used a broad, coarse acceleration search. The second trial extended the DM range to  $800 \text{ pc cm}^{-3}$  and had a very fine acceleration search. The third search used the archival data to target beams that contained high-mass X-ray binaries (HMXBs) in the LMC. These survey beams were then reprocessed using a very intensive acceleration search. New data were processed from a deep search of an X-ray point source in the SMC and a new high-resolution survey of the LMC using the Parkes Telescope.

### 2.1 Parkes Multibeam Survey

Archival data from the Parkes Multibeam Survey of the LMC and SMC were reprocessed and searched. The original observations took place between 2000 May and 2001 November. Using a centre frequency of 1374 MHz and a bandwidth of 288 MHz split into 96 channels, data were sampled every 1 ms for a total observing time of 8400 s per pointing (Manchester et al. 2006). Due to increased computing power and search algorithms, allowing us to use lower signal-to-noise ratios (S/N) and higher acceleration ranges (see Section 3), we were sensitive to lower luminosity and more highly accelerated pulsars than the Manchester et al. (2006) survey.

### 2.2 High-mass X-ray Binaries

The Magellanic Clouds have 128 catalogued HMXBs (Liu, van Paradijs & van den Heuvel 2005), and this provided a large sample of sources to search for corresponding radio pulsar signals with a uniform sensitivity. Multiwavelength detection of an HMXB as a radio pulsar provides insight into the evolution of these systems and into the physics of the companion star (see e.g. Thompson et al. 1994; Grove et al. 1995; pertaining to PSR B1259–63).

Despite extensive study of these HMXB systems (both in the Galaxy and in the Magellanic Clouds) at X-ray wavelengths as both persistent and as transient/bursting sources, only four radio pulsars have been found to date to be orbiting similarly high-mass, non-degenerate companions: PSRs J0045–7319 (itself in the SMC; Kaspi et al. 1994), J1638–4725 (Lyne 2008), J1740–3052 (Stairs et al. 2001) and B1259–63 (Johnston et al. 1992). Of these, only PSR B1259–63 is a member of a Be/X-ray binary system. Is it the case that accretion and/or eclipsing from the donor prevents radio emission from being detectable in many cases? Perhaps, but some HMXBs may be detectable as radio pulsars during the non-accretion phases of their orbits, if their orbits are sufficiently wide. PSR B1259–63 is one of these wide-orbit, eccentric systems, and it has been extensively studied as both a radio pulsar and transient

X-ray source since its discovery more than 20 yr ago (Johnston et al. 1992) particularly at or near its periastron passages, which occur every 3.4 yr. This system continues to provide exciting results using multiwavelength observations (see e.g. Chernyakova et al. 2009; Khangulyan et al. 2012; Kong, Cheng & Huang 2012).

HMXBs from the Magellanic Clouds HMXBs Catalog (Liu et al. 2005) were identified and checked for coincidence with the existing beams in the LMC and SMC radio surveys. These beams were then selected to run a directed search for radio emission using the Parkes Multibeam Survey data. Of the 128 HMXBs in the catalogue, 36 had positions that were either not in a coincident beam or found near the edge of a beam (therefore yielding low sensitivity), 16 were found in beams with excessive radio-frequency interference (RFI), which left 76 candidates to search. Since it is likely that a pulsar's signal would be highly accelerated, these beams were processed separately with a very fine acceleration search. Appendix A shows a list of all 76 HMXBs that were searched.

### 2.3 An SMC point source

We conducted a deep targeted radio search of SNR J0047.2–7308 which was centred on the X-ray point source identified within the supernova remnant (see Dickel et al. 2001). These observations were conducted to look for radio pulsations from a putative pulsar at that location. Two separate search observations of duration 5.3 and 5.6 h were conducted with the Parkes 64-m Radio Telescope in 2008 February. These observations used the centre beam of the multibeam receiver with a centre frequency of 1390 and 0.5 MHz filters giving a total bandwidth of 256 MHz (Manchester et al. 2001). The observing setup and the observations themselves were identical to the search observation reported in detail by Crawford et al. (2009) which targeted XTE J0103–728, with the exception of the integration times and the sampling time used. In the radio observations reported here, a sampling time of 80  $\mu\text{s}$  was employed to preserve sensitivity to millisecond pulsations from a young pulsar.

### 2.4 High-resolution LMC survey

New surveys of the LMC and SMC have recently been initiated using a new high-resolution backend, the Berkeley–Parkes–Swinburne data recorder (BPSR), located at the Parkes Telescope (Keith et al. 2010). These surveys were performed using the multibeam receiver at Parkes with a centre frequency of 1374 MHz and a bandwidth of 340 MHz. Each pointing was observed for 8600 s and the data were sampled every 64  $\mu\text{s}$  (see Ridley & Lorimer, in preparation). These surveys of the LMC and SMC began in 2009 May, and we plan to continue them until 2016. They are  $\sim 20$  per cent complete with 49 out of 209 pointings observed, and we report on the results to date.

## 3 DATA REDUCTION

The Parkes Multibeam data were searched multiple times with different search parameters. We first used the SIGPROC processing package<sup>1</sup> to search 60 DMs from 0 to  $300 \text{ pc cm}^{-3}$  using a minimum S/N of 9.0, and this search was sensitive to pulsars with periods from 10 ms to 10 s. A time-domain acceleration search, as implemented in the SIGPROC program `seek`, was performed over the range  $\pm 50 \text{ m s}^{-2}$

<sup>1</sup> <http://sigproc.sourceforge.net>

**Table 1.** List of newly discovered LMC pulsars, including the barycentred period, DM, epoch of discovery, integration time and discovery survey. PM refers to the Parkes Multibeam Survey of the Magellanic Clouds reprocessing, BPSR is the high-resolution survey and HMXB is the targeted search of HMXBs. Parentheses represent the uncertainty in the last digit quoted. Right ascension is given in units of hours, minutes and seconds, and the declination is given in units of degrees and arcminutes. The uncertainty in both RA and Dec. is  $\pm 7$  arcmin. The uncertainty in DM was determined using `prepold` plots, which is part of the `PRESTO` package.

PSR	RA (J2000)	Dec. (J2000)	$P$ (s)	DM ( $\text{pc cm}^{-3}$ )	EPOCH (MJD)	$T_{\text{int}}$ (s)	Survey	S/N
J0456–69	04 56 30	–69 10	0.117 073 051(15)	103(1)	52038	8300	PM	29.2
J0457–69	04 57 02	–69 46	0.231 390 388(73)	91(1)	55383	8600	BPSR	11.3
J0458–67	04 58 59	–67 43	1.133 9000(18)	97(2)	51810	8300	PM	10.8
J0521–68	05 21 44	–68 35	0.433 420 70(30)	136(4)	51871	8300	PM	19.3
J0532–69	05 32 04	–69 46	0.574 597 86(70)	124(1)	55420	7920	BPSR	9.6
J0535–66	05 35 40	–66 52	0.210 524 357(30)	75(1)	51393	14400	HMXB	7.1
J0537–69	05 37 43	–69 21	0.112 613 212(20)	273(1)	55420	7200	BPSR	8.5
J0542–68	05 42 35	–68 16	0.425 189 00(72)	114(5)	51975	3960	PM	18.6

using intervals of  $1 \text{ m s}^{-2}$ . Most pulsars in binary systems have accelerations up to  $5 \text{ m s}^{-2}$  (Camilo et al. 2000); however, some, such as PSR B1744–24A with  $a = 33 \text{ m s}^{-2}$  (Lyne et al. 1990), can be significantly greater. To minimize the drifting of the signal across multiple Fourier bins due to the trial acceleration differing from the true acceleration, we chose a step size so that  $\Delta a = cP/T_{\text{obs}}^2$ . With the 8400 s observations of the Parkes Multibeam Survey, the acceleration search was fully sensitive to all pulsars in binary systems having spin periods greater than 235 ms. The data were also searched for single bursts of radio emission having a pulse width between 64  $\mu\text{s}$  and 65 ms. A minimum flux density threshold for a single pulse search can be calculated (see Cordes & McLaughlin 2003) as

$$S_{\text{min}} = \frac{S_{\text{sys}}(S/N)_{\text{min}}}{W} \sqrt{\frac{W}{n_p \Delta f}}, \quad (1)$$

where  $W$  is pulse width,  $S_{\text{sys}}$  is the system equivalent flux density (34 Jy averaged across all beams of the multibeam receiver),  $n_p$  is the number of polarizations summed (2 for our case) and  $\Delta f$  is the receiver bandwidth. This made the search sensitive to giant bursts (of width 65 ms) having fluxes greater than 54 mJy.

A deeper search was also performed using the `SIGPROC` processing package and searched 160 DMs over a range of 0–800  $\text{pc cm}^{-3}$ . The Fourier S/N threshold used was 5.0, and all candidates above that were folded. However, after using the `PRESTO`<sup>2</sup> program `prepold`, only candidates with a resulting `prepold` sigma 8.0 and greater were inspected. This allowed us to detect a candidate that might appear weak in the FFT but was then enhanced in the fold. Since `SIGPROC` conducts an incoherent sum of the harmonics in the Fourier search, and the folded data are coherently summed, a pulsar candidate can improve its S/N significantly in the folded data and reveal an otherwise invisible pulsar. This method is, however, more computationally demanding. An acceleration search was also performed with a range between  $\pm 10 \text{ m s}^{-2}$  using intervals of  $0.1 \text{ m s}^{-2}$  which was fully sensitive to all pulsars with spin periods greater than 23.5 ms.

Survey beams containing the 76 HMXBs were searched using periodicity, single pulse and acceleration searches. DMs up to 800  $\text{pc cm}^{-3}$  (160 different DMs) were searched with candidates having S/N greater than 5.0 being considered. Accelerations between  $\pm 20 \text{ m s}^{-2}$  with step sizes of  $0.01 \text{ m s}^{-2}$  were tried, making this search fully sensitive to all binary pulsars having spin periods greater than 2.35 ms.

The pointed search observations of SNR J0047.2–7308 were analysed to look for a radio periodicity from a possible pulsar. After excision of RFI via the `PRESTO` program `rfifind`, each of the two data sets was dedispersed using a range of DMs from 0 to 800  $\text{pc cm}^{-3}$ , which easily encompassed the expected DM range for pulsars in the SMC (Manchester et al. 2006). Each separate dedispersed time series was Fourier transformed, and the resulting spectra were filtered and harmonically summed, then searched for candidate periodicities. Candidate signals were then checked by dedispersing and folding the data at DMs and periods near the candidate values. Each data set was also searched for dispersed impulsive signatures in case the source was an intermittent pulsar or rotating radio transient source (McLaughlin et al. 2006). The analysis closely followed the Fourier and single pulse search analysis of similar data described by Crawford et al. (2009). No promising candidates were found in the Fourier or single pulse search of either data set.

## 4 RESULTS

Four pulsars were discovered in the reprocessing of the Parkes Multibeam Survey of the Magellanic Clouds data, while one pulsar was found in the search of HMXBs. Three additional pulsars were found in the initial processing of the high-resolution LMC survey data. These pulsars were confirmed in separate observations at the Parkes Radio Telescope between 2011 January 14 and 2012 June 24. Some general properties of these eight new radio pulsars can be found in Table 1, while their time-resolved and integrated pulse profiles are shown in Fig. 1.

### 4.1 Properties of eight new pulsars

These eight new LMC pulsars encompass a wide range of periods and DMs. The periods range from 1.133 s for J0458–67 down to 112 ms for J0537–69. The 112 ms pulsar is the second shortest period known for a radio pulsar in the LMC after PSR B0540–69. It is also possible that it could be a young pulsar. Further timing observations are now planned for this and the other new discoveries.

The range of DMs of these pulsars is significant. Three of the newly discovered pulsars have DMs less than 100  $\text{pc cm}^{-3}$ . However, it is likely that they are all associated with the LMC since their DMs are all  $> 70 \text{ pc cm}^{-3}$ , higher than the four lowest DM pulsars in the LMC and well above the expected Galactic contribution to the DM in this direction ( $\sim 25 \text{ pc cm}^{-3}$ ; Cordes & Lazio 2002).

<sup>2</sup> <http://www.cv.nrao.edu/~sransom/presto>

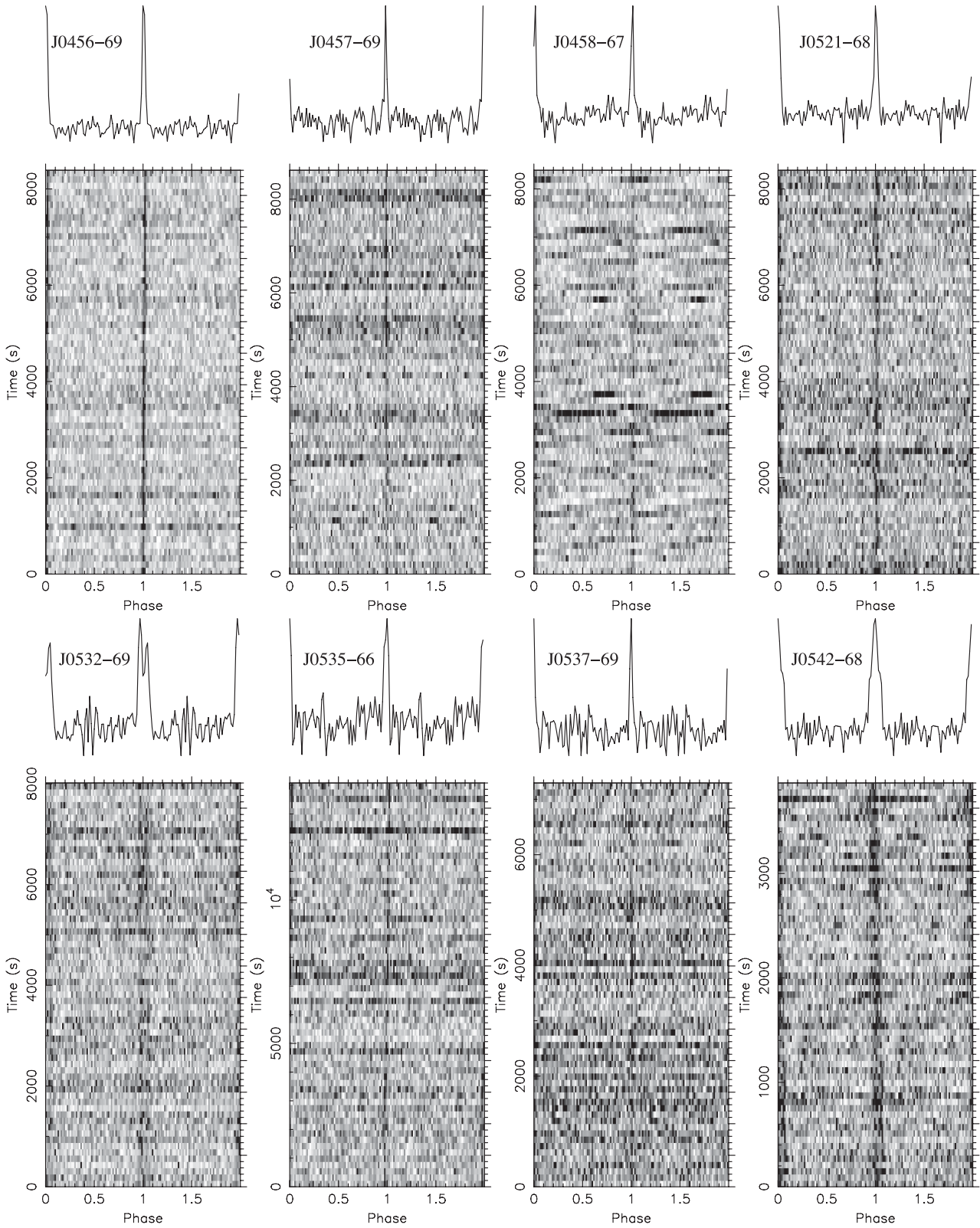


**Figure 1.** Discovery observations and integrated pulse profiles of the eight new LMC pulsars. For each pulsar, the grey-scale shows pulse intensity as a function of pulse phase and observation time. The sum of these data results in the integrated profile shown at the top of each plot. Two pulse phases are shown in each case for clarity.

PSR J0537–69, on the other hand, has a DM of  $273 \text{ pc cm}^{-3}$ . This is by far the highest DM of any known Magellanic Cloud pulsar (almost twice as high as the highest previously known DM of  $146 \text{ pc cm}^{-3}$  for PSR B0540) and indicates that it is likely the most distant LMC pulsar yet discovered.

#### 4.2 SNR J0047.2–7308

No radio pulses were observed from the point-like source in the SNR J0047.2–7308. The flux density limits on radio pulsations from the radio search depend on the period and duty cycle of any pulsations emitted by the source. For values that are typical for young pulsars (a 5 per cent duty cycle and a spin period that is between a few tens and a few hundreds of milliseconds), the 1400 MHz flux density upper limit to pulsed emission from the blind Fourier search is  $\sim 30 \mu\text{Jy}$ . For a distance of 60 kpc to the SMC (Hilditch, Howarth & Harries 2005) and assuming a 1 sr beaming fraction for any radio emission, this corresponds to a 1400 MHz radio luminosity of  $\sim 100 \text{ mJy kpc}^2$ . The limits on single-pulse emission are comparable to those reported for the radio search of XTE J0103–728 in the SMC (Crawford et al. 2009).

## 5 DISCUSSION

The known LMC pulsar population has now increased to 23 pulsars with the addition of these eight newly discovered pulsars. This is a 50 per cent increase in the total number of LMC pulsars. In this section, we discuss the DMs and flux densities of our new pulsars as compared to the previously known pulsars. Table 2 shows the properties of all currently known LMC pulsars.

### 5.1 Flux densities

A comparison of the flux densities of the previously discovered (from Manchester et al. 2006) and newly discovered pulsars is

**Table 2.** Complete list of all 23 known rotation-powered LMC pulsars.

PSR name	P (ms)	DM ( $\text{pc cm}^{-3}$ )	$S_{1400}$ (mJy)	Discovery paper
J0449–7031	479	65	0.14	Manchester et al. (2006)
J0451–67	245	45	0.05	Manchester et al. (2006)
J0455–6951	320	94	0.25	McConnell et al. (1991)
J0456–69	117	103	>0.15	This work
J0456–7031	800	100	0.05	Manchester et al. (2006)
J0457–69	231	91	>0.05	This work
J0458–67	1133	97	>0.07	This work
J0502–6617	691	68	0.25	McConnell et al. (1991)
J0519–6932	263	119	0.32	Manchester et al. (2006)
J0521–68	433	136	>0.12	This work
J0522–6847	674	126	0.19	Manchester et al. (2006)
J0529–6652	975	103	0.30	McCulloch et al. (1983)
J0532–6639	642	69	0.08	Manchester et al. (2006)
J0532–69	574	124	>0.05	This work
J0534–6703	1817	94	0.08	Manchester et al. (2006)
J0535–66	210	75	>0.03	This work
J0535–6935	200	89	0.05	Crawford et al. (2001)
J0537–69	112	273	>0.04	This work
J0537–6910	16	–	–	Marshall et al. (1998)
J0540–6919	50	146	0.02	Seward et al. (1984)
J0542–68	425	97	>0.14	This work
J0543–6851	708	131	0.22	Manchester et al. (2006)
J0555–7056	827	73	0.21	Manchester et al. (2006)

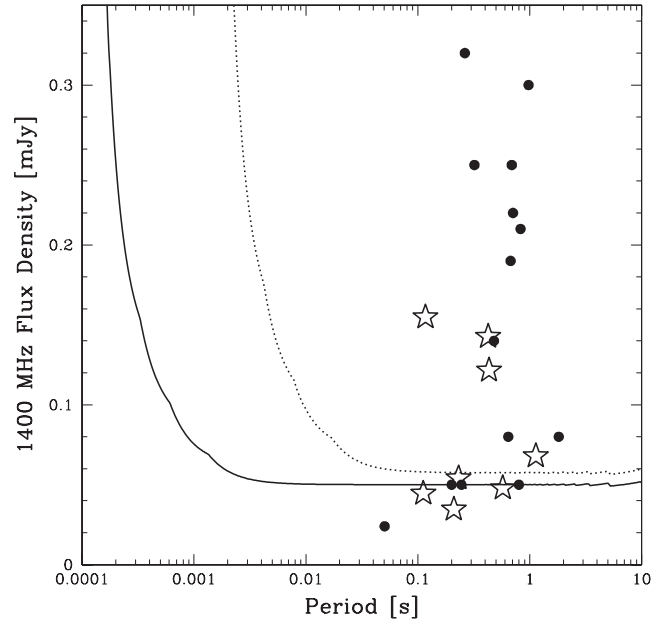


**Figure 2.** The 1400 MHz flux densities of all LMC pulsars are shown as a function of their pulse periods. The 14 previously known radio pulsars (PSR J0537–6910 is not included) are represented by filled circles while the eight new pulsars and the lower limits of their fluxes are denoted by stars. The dashed line corresponds to the minimum flux threshold of the Manchester et al. (2006) survey and the solid line is the minimum flux threshold of the new high-resolution SMC and LMC surveys as calculated following the procedure described in Manchester et al. (2001). The increased sensitivities of the new survey are due to the increase in bandwidth, decrease in sampling time and increase in the number of frequency channels. The two pulsars below the survey thresholds (PSRs B0540–69 and J0535–66) were discovered using longer integration times.

found in Fig. 2. We note that our improvements in computational power and search algorithms have enabled us to detect some pulsars with flux densities higher than the previous survey’s minimum flux. The flux values for the eight new pulsars were obtained via the radiometer equation,

$$S = \frac{T_{\text{sys}}(S/N)}{G \sqrt{n_p f_{\text{int}} \Delta f}} \sqrt{\frac{W}{P - W}}, \quad (2)$$

where  $G$  is the telescope gain,  $n_p$  is the number of polarizations summed,  $T_{\text{sys}}$  is the system temperature of the telescope, and  $W$  and  $P$  are the pulse width and period. For these calculations, we use  $G = 0.735 \text{ K Jy}^{-1}$  for the centre beam,  $G = 0.690 \text{ K Jy}^{-1}$  for the inner ring,  $G = 0.581 \text{ K Jy}^{-1}$  for the outer ring (see Manchester et al. 2001),  $n_p = 2$  and  $T_{\text{sys}} = 24 \text{ K}$ . The pulse width,  $W$ , is assumed to be  $0.05 P$ . Since the pulsars’ positions are only known to be within the beam radius, these quoted values are actually lower limits on their flux measurements.

### 5.2 Dispersion measures

Most of the pulsars in both the LMC and SMC have DMs within the range of  $65\text{--}150 \text{ pc cm}^{-3}$  (Manchester et al. 2006). PSR J0537–69 was discovered to have a DM of  $273 \text{ pc cm}^{-3}$  which makes it the most highly dispersed pulsar located in the direction of the LMC and probably the most distant. The DMs of all LMC pulsars (with the exception of the X-ray pulsar, J0537–6910) are plotted in Fig. 3.

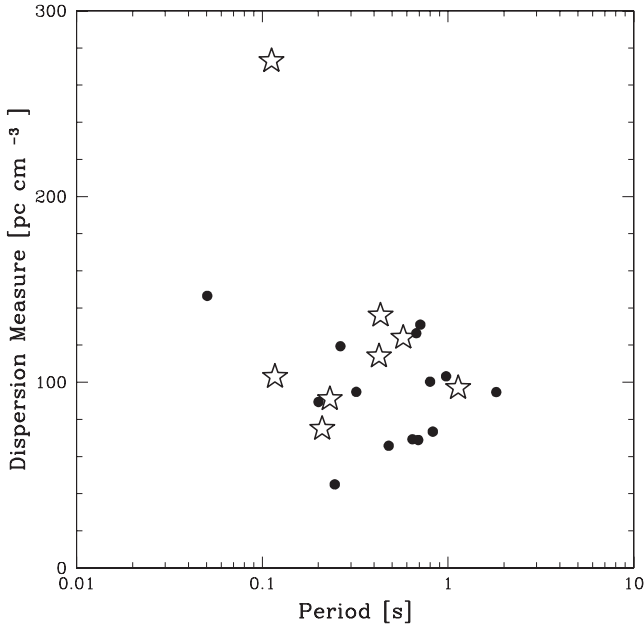


**Figure 3.** The DMs of all LMC pulsars (with the exception of J0537–6910, which has not been radio detected) are displayed as a function of spin period. The filled circles represent previously known pulsars and the stars correspond to the new discoveries.

### 5.3 The population of LMC pulsars

Using the current sample of pulsars in the LMC, we applied the Bayesian techniques developed by Chennamangalam et al. (2013) to constrain the number of potentially detectable LMC pulsars. Here, we take prior knowledge of the flux densities of the LMC pulsars and the mean and standard deviation ( $\mu$  and  $\sigma$ ) of the log-normal luminosity function (Faucher-Giguère & Kaspi 2006), the use of which is justified below in Section 5.4, to determine the population size ( $N$ ). We follow the procedure and used the code detailed in Chennamangalam et al. (2013) to carry out this analysis. Since the diffuse radio flux of the LMC is not uniquely connected to the pulsar population, our analysis did not make use of the techniques described in section 2.3 of Chennamangalam et al. (2013), where the diffuse flux of the millisecond pulsars is used to constrain globular cluster pulsar populations. The X-ray pulsar, J0537–6910, does not have a measured radio flux and hence is not included in our analysis. Likewise, two pulsars (J0535–6935 and B0540–6919) were detected in targeted searches using much longer integration times than the surveys discussed here. They were also excluded yielding a total of 20 pulsars for this analysis.

We assumed a distance of  $49.97 \pm 1.3$  kpc to the LMC (Pietrzyński et al. 2013) and a minimum survey sensitivity of 0.05 mJy. Following Boyles et al. (2011), we used the results of Ridley & Lorimer (2010a) to constrain the luminosity function priors to be flat in the ranges  $-1.19 < \mu < -1.04$  and  $0.91 < \sigma < 0.98$ . This results in a posterior probability-density function (see Fig. 4) for the total number of potentially observable pulsars with a median of  $57\,000^{+70\,000}_{-30\,000}$ , where the upper and lower limits are given by a 95 per cent credible interval.

In an effort to further explore the luminosity function and underlying pulsar population, we also tried a wide range of priors for  $\mu$  and  $\sigma$ . In this analysis, we allowed  $\mu$  to vary between  $-2.0$  and  $0.5$  and  $\sigma$  to vary between  $0.2$  and  $1.4$  according to Bagchi, Lorimer & Chennamangalam (2011). The resulting constraints on the number

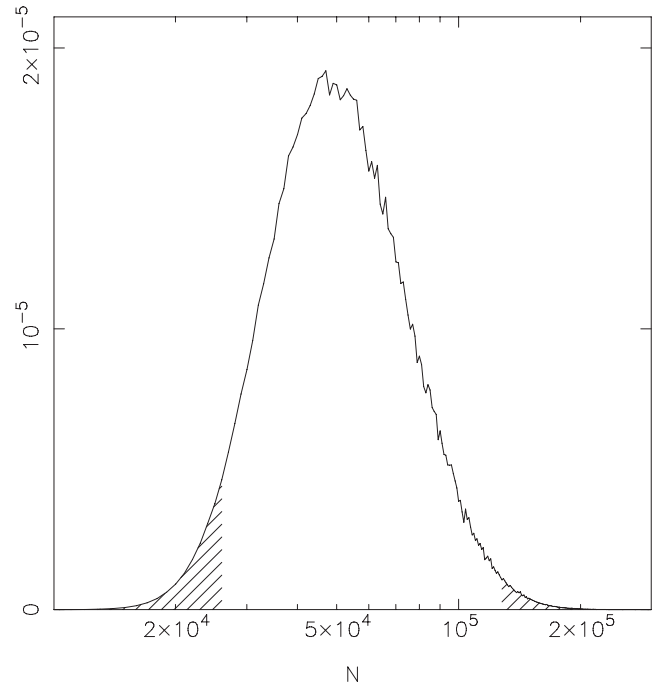


**Figure 4.** The posterior probability-density function for the total number of potentially observable pulsars. The hatched areas represent regions outside of the 95 per cent credible interval.

**Table 3.** Median values for  $N$ ,  $\mu$  and  $\sigma$  for our Bayesian analysis of the LMC pulsar population and luminosity function. For the narrow priors case, the quoted values for  $\mu$  and  $\sigma$  only represent the range of priors that were used in the analysis.

	$N$	$\mu$	$\sigma$
WIDE	$21\,000^{+71\,000}_{-20\,000}$	$-1.55^{+1.55}_{-0.45}$	$1.14^{+0.22}_{-0.28}$
NARROW	$57\,000^{+70\,000}_{-30\,000}$	$-1.12^{+0.07}_{-0.07}$	$0.95^{+0.03}_{-0.04}$

of pulsars and the luminosity function are summarized in Table 3. The constraints on the total number of pulsars for these wide priors are consistent with the narrow prior results, albeit with large uncertainties. The currently observed population of LMC pulsars is not large enough to uniquely constrain the shape of the pulsar luminosity function. More sensitive surveys with future instruments would undoubtedly help to sample the fainter regions of the luminosity function and result in tighter constraints.

### 5.4 Luminosity distribution

The above analysis assumes the log-normal luminosity distribution found from the studies of Galactic pulsars (Faucher-Giguère & Kaspi 2006). An interesting question to address with the growing sample of pulsars in the LMC is whether their luminosity distribution is indeed consistent with the Galactic population. To quantify this, we approximate the high-luminosity tail of the distribution as a power law, where the number of pulsars ( $N$ ) as a function of the luminosity ( $L$ ) can be written as follows:

$$\log N = \alpha \log L + C. \quad (3)$$

Here,  $C$  is a constant and  $\alpha$  represents the slope of the distribution (Lorimer et al. 2006). We obtain a slope of  $\alpha = -1.2$  for Galactic pulsars with  $L > 30$  mJy kpc<sup>2</sup>, and a slope of  $\alpha = -3.6$  for LMC

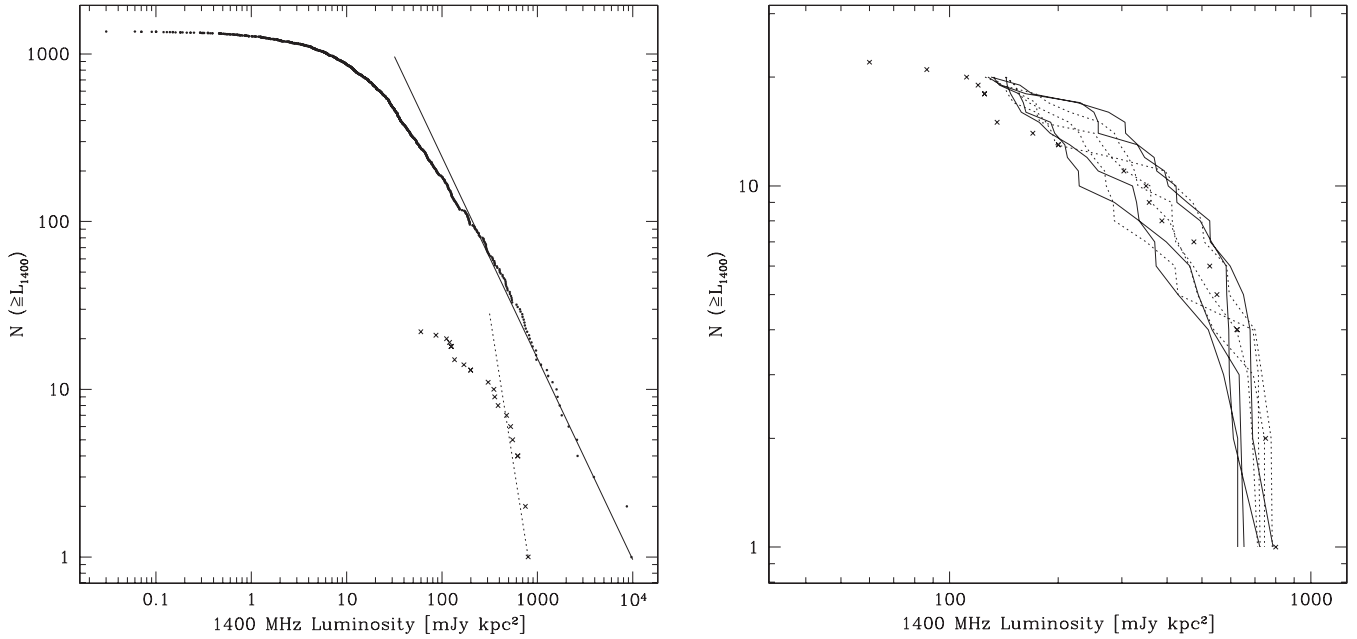


**Figure 5.** The CDF for both Galactic and LMC pulsars. The left plot shows the Galactic pulsars (dots) and power-law fit of  $\alpha = -1.2$  and the LMC pulsars (represented by an X) with the corresponding power-law fit of  $\alpha = -3.6$ . The right plot shows only the LMC pulsars with four simulated populations using the power-law distribution (solid lines) and four simulated populations using the log-normal distribution (dotted lines).

pulsars with  $L > 125 \text{ mJy kpc}^2$  (see Fig. 5). At first glance, then, it appears that the slope and maximum luminosity of the two samples are markedly different.

To investigate this apparent discrepancy between the Galactic and LMC luminosity distributions, we simulated the luminosities of pulsars found in the LMC and compared them with the observed distribution. We first generated 20 pulsars using a power-law model with  $\alpha = -1.2^3$  and plotted the resulting cumulative distribution function (CDF) along with the actual observed luminosities. We then simulated another set of 20 pulsars using the log-normal luminosity function values of  $\mu = -1.1$  and  $\sigma = 0.9$  (Faucher-Giguère & Kaspi 2006). We ran four trials of each simulation type and plotted the results in Fig. 5. As can be seen, the luminosities of the simulated pulsars do not vary significantly from the observed luminosities. We conclude that, given the present statistics, the luminosity function of normal pulsars in the LMC is consistent with that of their counterparts in the Galaxy. Our assumption of the log-normal luminosity function in the previous section therefore appears to be completely justified by the present sample. We attribute the steeper slope of the observed LMC pulsars as a bias due to the smaller sample size. The higher maximum luminosity seen for Galactic pulsars may be due in part to significant distance uncertainties associated with the Cordes & Lazio electron-density model which are not present in the LMC sample due to our adoption of a common distance from Pietrzyński et al. (2013). A cap on the luminosity distribution, based on the LMC sample, seems to be approximately  $1000 \text{ mJy kpc}^2$ .

### 5.5 Small Magellanic Cloud

Our reprocessing also searched the areas of the sky populated by the SMC. However, no new pulsars were detected. The smaller size of the cloud inherently leads to a fewer number of stars being present;

hence the likelihood of detecting a pulsar is diminished. Ridley & Lorimer (2010b) estimated that there are 40 per cent fewer pulsars in the SMC than in the LMC, or  $N_{\text{SMC}} = 0.6N_{\text{LMC}}$ . Further decreasing our odds of a new discovery is the increased distance to the SMC of 60 kpc (Hilditch et al. 2005). Since  $S = L \times d^2$ , the observed flux of an SMC pulsar as compared to an LMC pulsar is given by  $S_{\text{SMC}} = S_{\text{LMC}} \left(\frac{49.97}{60}\right)^2$ , meaning that the observed flux is reduced by 31 per cent. The five currently known SMC pulsars are the most distant pulsars confirmed to date.

## 6 CONCLUSIONS

With the eight new pulsars presented in this work there are now 23 known spin-powered pulsars known in the LMC, representing a 50 per cent increase in the population. Based on these results, using a Bayesian analysis, we constrain the total population of potentially observable pulsars in the LMC to be  $57\,000^{+70\,000}_{-30\,000}$  (95 per cent credible interval). The luminosity function of LMC pulsars is consistent with that of normal pulsars in the Galaxy. Our results suggest that the maximum 1400 MHz radio luminosity is  $1000 \text{ mJy kpc}^2$ . Further work is being done to complete the high-resolution BPSR survey of the LMC with the goal of establishing a deep and comprehensive survey of the entire galaxy. We hope to further increase the total number of known LMC pulsars and find the first extragalactic millisecond pulsars (see e.g. Ridley & Lorimer 2010b).

We are also conducting a BPSR survey of the SMC (Ridley & Lorimer, in preparation) to find fainter and more rapidly rotating pulsars in that galaxy. After observing 12 out of 73 planned pointings, no new pulsars have been detected, but a similar goal of performing an exhaustive search for pulsars in the SMC exists.

## ACKNOWLEDGEMENTS

The Parkes Radio Telescope is part of the Australia Telescope which is funded by the Commonwealth of Australia for operation as a

<sup>3</sup> Similar results are found if we adopt a flatter slope of  $\alpha = -0.7$  as found by Lorimer et al. (2006).

National Facility managed by CSIRO. We thank Andrew Jame-son, Matthew Bailes and Mike Keith for assistance with the BPSR data acquisition system. This work made use of the facilities of the ATNF Pulsar Catalogue. Summer support for SRB and computer resources at WVU used during this project were made possible by a WV EPSCoR Challenge Grant. DRL acknowledges support from the Research Corporation for Scientific Advancement as a Cottrell Scholar and current support from Oxford Astrophysics while on sabbatical leave. Student work at F&M was supported by the Hackman scholarship fund. We also thank the referee, Matthew Bailes, for helpful comments.

## REFERENCES

- Bagchi M., Lorimer D. R., Chennamangalam J., 2011, MNRAS, 418, 477  
 Boyles J., Lorimer D. R., Turk P. J., Mnatsakanov R., Lynch R. S., Ransom S. M., Freire P. C., Belczynski K., 2011, ApJ, 742, 51  
 Burgay M. et al., 2006, MNRAS, 368, 283  
 Camilo F., Lorimer D. R., Freire P., Lyne A. G., Manchester R. N., 2000, ApJ, 535, 975  
 Chennamangalam J., Lorimer D. R., Mandel I., Bagchi M., 2013, MNRAS, 431, 874  
 Chernyakova M., Neronov A., Aharonian F., Uchiyama Y., Takahashi T., 2009, MNRAS, 397, 2123  
 Cordes J. M., Lazio T. J. W., 2002, preprint (astro-ph/020715)  
 Cordes J. M., McLaughlin M. A., 2003, ApJ, 596, 1142  
 Crawford F., Kaspi V. M., Manchester R. N., Lyne A. G., Camilo F., D'Amico N., 2001, ApJ, 553, 367  
 Crawford F., Lorimer D. R., Devour B. M., Takacs B. P., Kondratiev V. I., 2009, ApJ, 696, 574  
 Dickel J. R., Williams R. M., Carter L. M., Milne D. K., Petre R., Amy S. W., 2001, AJ, 122, 849  
 Eatough R. P., Kramer M., Lyne A. G., Keith M. J., 2013, MNRAS, 431, 292  
 Edwards R. T., Bailes M., van Straten W., Britton M. C., 2001, MNRAS, 326, 358  
 Faucher-Giguère C.-A., Kaspi V. M., 2006, ApJ, 643, 332  
 Grove E., Tavani M., Purcell W. R., Kurfess J. D., Strickman M. S., Arons J., 1995, ApJ, 447, L113  
 Hilditch R. W., Howarth I. D., Harries T. J., 2005, MNRAS, 357, 304  
 Jacoby B. A., Bailes M., van Kerkwijk M. H., Ord S., Hotan A., Kulkarni S. R., Anderson S. B., 2003, ApJ, 599, L99  
 Johnston S., Manchester R. N., Lyne A. G., Bailes M., Kaspi V. M., Qiao G., D'Amico N., 1992, ApJ, 387, L37  
 Kaspi V. M., Johnston S., Bell J. F., Manchester R. N., Bailes M., Bessell M., Lyne A. G., D'Amico N., 1994, ApJ, 423, L43  
 Keith M. J., Eatough R. P., Lyne A. G., Kramer M., Possenti A., Camilo F., Manchester R. N., 2009, MNRAS, 395, 837  
 Keith M. J. et al., 2010, MNRAS, 409, 619  
 Khangulyan D., Aharonian F. A., Bogovalov S. V., Ribó M., 2012, ApJ, 752, L17  
 Knispel B. et al., 2013, preprint (astro-ph/1302.0467)  
 Kong S. W., Cheng K. S., Huang Y. F., 2012, ApJ, 753, 127  
 Liu Q. Z., van Paradijs J., van den Heuvel E. P. J., 2005, A&A, 442, 1135  
 Lorimer D. R. et al., 2006, MNRAS, 372, 777  
 Lyne A. G., 2008, in Bassa C., Wang Z., Cumming A., Kaspi V. M., eds, AIP Conf. Ser., Vol. 983, Parkes 20-cm Multibeam Pulsar Surveys. Am. Inst. Phys., New York, p. 561  
 Lyne A. G., Johnston S., Manchester R. N., Staveley-Smith L., D'Amico N., 1990, Nat, 347, 650  
 McConnell D., McCulloch P. M., Hamilton P. A., Ables J. G., Hall P. J., Jacka C. E., Hunt A. J., 1991, MNRAS, 249, 654  
 McCulloch P. M., Hamilton P. A., Ables J. G., Hunt A. J., 1983, Nat, 303, 307  
 McLaughlin M. A. et al., 2006, Nat, 439, 817  
 Manchester R. N. et al., 2001, MNRAS, 328, 17  
 Manchester R. N., Fan G., Lyne A. G., Kaspi V. M., Crawford F., 2006, ApJ, 649, 235  
 Marshall F. E., Gotthelf E. V., Zhang W., Middleditch J., Wang Q. D., 1998, ApJ, 499, L179  
 Mickaliger M. B. et al., 2012, ApJ, 759, 127  
 Pietrzyński G. et al., 2013, Nat, 495, 76  
 Ridley J. P., Lorimer D. R., 2010a, MNRAS, 404, 1081  
 Ridley J. P., Lorimer D. R., 2010b, MNRAS, 406, L80  
 Seward F. D., Harnden F. R., Jr, Helfand D. J., 1984, ApJ, 287, L19  
 Stairs I. H. et al., 2001, MNRAS, 325, 979  
 Staveley-Smith L. et al., 1996, PASA, 13, 243  
 Thompson C., Blandford R. D., Evans C. R., Phinney E. S., 1994, ApJ, 422, 304

## APPENDIX A: HIGH-MASS X-RAY BINARIES SEARCHED FOR RADIO PULSATIONS IN THE LMC AND SMC

**Table A1.** Catalogue of 76 HMXBs in the LMC and SMC searched for radio pulsations and dispersed radio bursts. The X-ray type refers to whether the source is a pulsar (P), transient X-ray source (T), or ultrasoft X-ray spectrum (U) (see Liu et al. 2005). The RA is given in units of hours, minutes and seconds, and the Dec. is given in units of degrees, arcminutes and arcseconds.

Name	RA (J2000)	Dec. (J2000)	Orbital period (d)	X-ray type	Spect. type	Spin period (s)	Alt name
RX J0032.9–7348	00 32 56.10	–73 48 19.0			Be		
RX J0041.2–7306	00 41 16.40	–73 06 41.0					
AX J0042.0–7344	00 42 04.80	–73 44 58.0					
RX J0045.6–7313	00 45 37.90	–73 13 54.0			Be		
RX J0047.3–7312	00 47 23.42	–73 12 27.3	48.800	P	B2e	263.6400	AX J0047.3–7312
AX J0048.2–7309	00 48 14.90	–73 10 03.0			Be		
RX J0048.5–7302	00 48 34.50	–73 02 30.0			Be		XMMU J004834.5–730230
RX J0049.2–7311	00 49 13.84	–73 11 36.7		P	Be	9.1321	XMMU J004913.8–731136
RX J0049.5–7310	00 49 29.92	–73 10 58.0	91.500		Be		XMMU J004929.9–731058
RX J0049.7–7323	00 49 42.00	–73 23 15.0	394.000	P	B1-3Ve	755.5000	XMMU J004942.3–732313
XTE J0050–732#1	00 50 00.00	–73 16 00.0	189.000	P		16.6000	
XTE J0050–732#2	00 50 00.00	–73 16 00.0		P		51.0000	
RX J0050.7–7316	00 50 44.70	–73 16 05.0	1.416	P	B0III-Ve	323.0000	AX J0051–733
RX J0050.9–7310	00 50 57.60	–73 10 07.9			Be		AX J0050.8–7310
XTE SMC46	00 51 00.00	–73 18 00.0		TP		46.4000	
RX J0051.3–7250	00 51 19.60	–72 50 44.0			Be		
AX J0051.4–7227	00 51 25.40	–72 27 29.0					



Table A1 – *continued*

Name	RA (J2000)	Dec. (J2000)	Orbital period (d)	X-ray type	Spect. type	Spin period (s)	Alt name
AX J0051.6–7302	00 51 39.90	–73 02 58.0					
XTE J0051–727	00 51 42.00	–72 45 00.0		TP		293.9000	
RX J0051.9–7255	00 51 54.20	–72 55 36.0			Be		
XTE J0052–725	00 52 09.10	–72 38 03.0		TP		82.4000	
2E0051.1–7304	00 52 52.40	–72 48 30.0			B0e		
RX J0052.9–7158	00 52 59.20	–71 57 58.0	200.000	TPU	Be	169.3000	2E 0051.1–7214
CXOU J005323.8–722715	00 53 23.80	–72 27 15.0	125.000	P	Be	138.0000	RX J0053.4–7227
XTE SMC95	00 53 24.00	–72 49 18.0	280.000	TP		95.0000	
XTE Position A	00 53 54.00	–72 26 42.0		P		89.0000	
1WGA J0053.8–7226	00 53 55.00	–72 26 47.0	139.000	TP	B1-B2III-Ve	46.6300	XTE J0053–724
RX J0054.5–7228	00 54 33.20	–72 28 09.0			Be		
H 0053–739	00 54 36.20	–73 40 35.0		TP	B1.5Ve	2.3700	SMC X-2
AX J0054.8–7244	00 54 55.88	–72 45 10.5	261.000	TP	O9Ve	503.5000	RX J0054.9–7245
XTE J0055–724	00 54 56.17	–72 26 27.6	123.000	TP	B0-B1III-V	58.9690	1SAX J0054.9–7226
XMMU J005517.9–723853	00 55 18.44	–72 38 51.8		P	O9V	701.6000	RX J0055.2–7238
XTE J0055–727	00 55 24.00	–72 42 00.0	34.800	TP		18.3700	
CXOU J005527.9–721058	00 55 27.70	–72 10 59.0		P		34.0800	RX J0055.4–7210
XMMU J005605.2–722200	00 56 05.24	–72 22 00.9		P	Be	140.1000	2E0054.4–7237
XMMU J005615.2–723754	00 56 15.20	–72 37 54.0			Be		
XMMU J005724.0–722357	00 57 24.00	–72 23 57.0					
AX J0057.4–7325	00 57 26.80	–73 25 02.0		P		101.4500	RX J0057.4–7325
CXOU J005736.2–721934	00 57 36.20	–72 19 34.0	95.300	P	Be	564.8300	XMMU J005735.7–721932
RX J0057.8–7202	00 57 48.40	–72 02 42.0		P	Be	280.4000	AX J0058–7203
CXOU J005750.3–720756	00 57 50.30	–72 07 56.0		P		152.1000	RX J0057.8–7207
RX J0058.3–7216	00 58 20.70	–72 16 18.0					AX J0058.3–7217
RX J0059.2–7138	00 59 11.30	–71 38 45.0		TUP	B1IIIe	2.7632	
1XMMU J005921.0–722317	00 59 21.04	–72 23 16.7		P	B0	202.0000	RX J0059.3–7223
XMMU J010030.2–722035	01 00 30.23	–72 20 35.1			Be		
RX J0101.6–7204	01 01 37.56	–72 04 18.7			Be		
XTE J0103–728	01 03 24.00	–72 43 00.0		TP		6.8482	
RX J0103.6–7201	01 03 37.57	–72 01 33.2		P	O5Ve	1323.2000	
RX J0104.5–7221	01 04 35.60	–72 21 43.0		T	Be		
RX J0105.7–7226	01 05 41.60	–72 26 17.0					XMMU J010541.5–722617
AX J0113.0–7246	01 13 05.50	–72 46 25.0					
RX J0117.6–7330	01 17 41.40	–73 30 49.0		TP	B0.5IIIe	22.0700	
AX J0127.8–7307	01 27 48.00	–73 07 39.0					
RX J0456.9–6824	04 56 54.10	–68 24 35.0					
RX J0457.2–6612	04 57 12.40	–66 12 10.0					
RX J0501.6–7034	05 01 23.90	–70 33 33.0			B0Ve		CAL 9
RX J0502.9–6626	05 02 51.60	–66 26 25.0		TP	B0Ve	4.0635	CAL E
RX J0512.6–6717	05 12 41.80	–67 17 23.0					
RX J0524.2–6620	05 24 12.70	–66 20 50.0					
RX J0527.3–6552	05 27 23.70	–65 52 35.0					
RX J0529.4–6952	05 29 25.90	–69 52 11.0					
RX J0529.8–6556	05 29 48.40	–65 56 51.0		TP	B0.5Ve	69.5000	
RX J0531.2–6607	05 31 13.80	–66 07 03.0	25.400	TP	B0.7Ve	13.7000	EXO 053109–6609.2
RX J0531.5–6518	05 31 36.10	–65 18 16.0			B2V		
RX J0532.4–6535	05 32 25.30	–65 35 09.0					
2A 0532–664	05 32 46.10	–66 22 03.0	1.400	P	O8 III	13.5000	LMC X-4
RX J0535.0–6700	05 35 05.90	–67 00 16.0	241.000	T	B0Ve		
1A 0535–668	05 35 41.20	–66 51 52.0	16.700	PT	B0.5 IIIe	0.0690	1A 0538–66
RX J0535.6–6651	05 35 41.60	–66 51 58.0					
RX J0535.8–6530	05 35 53.80	–65 30 34.0					
1H 0538–641	05 38 56.30	–64 05 03.0	1.700	U	B2.5 Ve		LMC X-3
XMMU J054134.7–682550	05 41 34.70	–68 25 50.0					
RX J0541.5–6833	05 41 37.10	–68 32 32.0			B0III		RX J0541.6–6832
1SAX J0544.1–7100	05 44 06.30	–71 00 50.0	286.000	TP	B0Ve	96.0800	RX J0544.1–7100
H 0544–665	05 44 15.60	–66 34 59.0			B0 Ve		
RX J0546.8–6851	05 46 48.30	–68 51 47.0					